Draft version May 14, 2021
Typeset using LaTeX **twocolumn** style in AASTeX63

Two New Black Widow Millisecond Pulsars In M28

Andrew Douglas[1]

[1] *University of Virginia*
1826 University Ave
Charlottesville, VA 22904, USA

(Received May 14, 2021)

Submitted to University of Virginia Astronomy Department Thesis Review

ABSTRACT

We report the discovery of two new black widow millisecond pulsars in the globular cluster M28 with the MeerKAT telescope. J1824−2452M (M28M) is a 4.78 ms pulsar in a 4 hour orbit. J1824-2452N (M28N) is a 3.35-ms pulsar with a 4.45 hour orbit. Both pulsars are at a dispersion measure of 119.30 pc cm^{-3} and appear to be black widow systems which do not show strong eclipses or orbital variation. We expect additional pulsars will be found in M28 with more sensitive observations.

Keywords: M28 – Pulsar – PRESTO – Jerk Search – MeerKAT

1. INTRODUCTION

Globular clusters (GCs) are a rich environment for the creation of millisecond pulsars (MSPs; Ransom 2008). The fast spin periods of MSPs are due to the accretion of mass and angular momentum from companion stars. Due to the stellar density in the central regions of globular clusters, the frequency of stellar interactions produces dynamically-formed binaries that can spin up a neutron star member. Additionally, these dynamical encounters can produce MSPs in highly eccentric and exotic orbits. Because of the high likelihood of finding millisecond pulsars (especially those in exotic orbits), many globular clusters have been searched deeply for pulsars with the largest radio telescopes. There are 39 pulsars currently discovered in Terzan 5 (Ransom et al. 2005) and 27 in 47 Tucanae (Camilo et al. 2000). M28 had, up until this point, 12 known pulsars (Bégin 2006) making it the cluster with the third most known. It had the first globular cluster pulsar discovered in 1987 (PSR B1821−24 or M28A; Lyne et al. 1987), as well as a transitional MSP that behaves alternatively as a radio MSP and as an active x-ray binary (IGR J18245–2452 or M28I; Papitto et al. 2013).

M28 has been the subject of many multi-wavelength searches in the past few decades. In 1994 the ROSAT x-ray telescope observed M28A as a possible x-ray source (Danner et al. 1994). In 2002, and multiple times since, M28 was observed by the *Chandra X-ray Observatory* (Bogdanov et al. 2011). In 2005, the Green Bank Telescope observed M28 and detected 11 new radio MSPs (Bégin 2006).

M28 is also known to be home to a disproportionately large percentage of black-widow pulsars. "Black-Widow" systems refer to binaries where the companion star (to the MSP) is of a low mass ($\leq 0.04\, M_{\odot}$) and an orbit of a few hours (Roberts 2013).

The MeerKAT telescope is a newly commissioned 64-dish telescope array in South Africa. The MeerKAT survey chose specific clusters that had been searched before for the purposes of comparing older detections with newer MeerKAT detections (Ridolfi et al. 2021). With 15 years since the last dedicated searches (using the GBT), the highly-sensitive MeerKAT telesocpe, and the addition of a jerk search capability in `PRESTO` (Andersen & Ransom 2018), we expected to find at least one new pulsar.

In this paper we present discoveries and timing of M28M and M28N. In section 2 we present the observation and discovery of the MSPs and the timing procedure. In section 3 we discuss the implications of the discovery and in section 4 we discuss our conclusions.

ard5yx@virginia.edu

2. OBSERVATIONS AND DATA ANALYSIS

2.1. *Data*

The initial MeerKAT data that we used to search for new pulsars in M28 was part of the series of survey observations using the core MeerKAT antennas that targeted globular clusters with known pulsars (Ridolfi et al. 2021). These observations were made as part of a joint effort of the MeerTime project (Bailes et al. 2020), which concentrates on long-term pulsar timing, and the TRAPUM project[1] (TRansients And PUlsars with MeerKAT), whose goal is to discover new pulsars.

The MeerKAT teams surveyed nine globular clusters, each of which had at least one known pulsar, for the purposes of comparing performance between the MeerKAT observations and those of other telescopes. Southern clusters, especially those that had only been searched using the Parkes Telescope, were prioritized given the large expected sensitivity improvements of MeerKAT.

The two 9000-second duration MeerTime observations occurred on 2019 July 19 and 2020 February 4, with 642 MHz of bandwidth centered at 1283.58 MHz. The 768 frequency channels were coherently dedispersed at a dispersion measure (DM) of 119.892 $\mathrm{pc\,cm^{-3}}$, which is roughly the average value of the DMs of the known pulsars in the cluster, and were subsequently further integrated into 256 channels with a sampling time of $\sim$76.56 μs. In addition to the two MeerTime observations, we had access to the central beams of two four-hour TRAPUM observations taken on 2020 December 6 and 11, which were not coherently dedispersed but had 2048 frequency channels over 856 MHz of bandwidth centered at 1283.86 MHz. As with the MeerTime data, these observations were later partially dedispersed into 256 frequency channels and integrated in time to $\sim$76.56 μs samples for analysis.

2.2. *Searches*

We used `PRESTO` to perform Fourier domain acceleration and jerk searches on the M28 data using its routine `accelsearch` (Ransom 2001). The jerk search functionality was a relatively recent addition to `PRESTO` (Andersen & Ransom 2018). Jerk searching aims to find pulsars whose accelerations are changing linearly. These signals are found from pulsars in compact binary orbits, and jerk searches improve our sensitivity to such systems (Bagchi et al. 2013).

We searched a range of dispersion measures (DMs) from 115.0 $\mathrm{pc\,cm^{-1}}$ to 125.0 $\mathrm{pc\,cm^{-1}}$, with a step size of 0.1 $\mathrm{pc\,cm^{-1}}$. We chose this range as it was roughly centered on the average DM of the pulsars in the cluster. It would be unlikely that we would find any millisecond pulsars outside this range. We conducted various levels of searches. We mostly searched with `-zmax 200 -wmax 600` and `-zmax 300 -wmax 900`. We also conducted short chunk searches at on the MeerTime data at 29 and 58 million points: around one third (50 minutes) and two thirds (100 minutes) of the 117 million point data file respectively. With the TRAPUM data we conducted short chunk searches at 45 and 90 million points, very roughly one quarter and one half of the 187 million point data file respectively. Both pulsars were found using the short-chunk functionality .

We first searched M28 with acceleration only, `-zmax 200`, hoping to find a pulsar through MeerKAT's increased sensitivity. We conducted a full search and a short-chunk search, however did not find any stand-out candidates. We next upgraded to jerk searching, with `-zmax 200` and `-wmax 600`. In the full search we were able to detect M28M at the DM 119.30 on the July 19 2019 data file of the MeerKAT observation at z=19.50 and w=10. We were unable to blindly detect the pulsar in the February 4 of 2020 observation so we had to use the TRAPUM observations from December 6th and 11th of 2020. We were able to confirm M28M in these data. We continued searching TRAPUM and MeerTime data at `-zmax 200` and `-wmax 600`. We soon detected a second candidate that we confirmed to be M28N at z=3 and w=60 in the February 4 2020 data. Since both pulsars were detected in the center TRAPUM beams (about 416 mas across) we know they are close to the center of the cluster.

2.3. *Timing*

With multiple detections of both new pulsars over the four MeerKAT observations, we were able to determine circular orbits and average barycentric spin periods for each pulsar using `PRESTO`'s `fit_circular_orbit.py` routine. These initial ephemerides allowed us to iteratively fold, detect, and determine pulse arrival times from the large number of archival observations of M28 from the Green Bank Telescope (GBT), starting in 2005 and continuing to the present day.

The GBT data from 2005 to 2008 was a mixture of L-band (centered at 1500 MHz) and S-band (centered at 2 GHz) observations using the Pulsar Spigot (Kaplan et al. 2005) and having effectively $\sim$600 MHz of available bandwidth with 1536 frequency channels sampled every 81.92 μs (see Bégin 2006, for more details). Starting in 2010 and continuing through mid-2020, observations were made with the Green Bank Ultimate Pulsar Processing Instrument (GUPPI; DuPlain et al. 2008), using the same bands, but with 512 coherently dedispersed channels, since then partially integrated to 128 chan-

[1] TRAPUM: http://trapum.org

nels with 40.96 μs sampling. Finally, for the past year, we used VEGAS (Bussa & VEGAS Development Team 2012), in an identical mode to the GUPPI observations.

Both the new pulsars were detected, albeit often with very low signal-to-noise (sometimes approaching unity), in the vast majority of the archival GBT observations. The total GBT integration time, sampled roughly quarterly, is 49.6 hours at L-band and 73.8 hours at S-band.

We determined times of arrival (TOAs) for each pulsar using the `get_TOAs.py` routine in `PRESTO` after fitting gaussians to the highest signal-to-noise TRAPUM observation (see Fig. 1) to use as noiseless pulse templates. We were typically able to get roughly one TOA per hour of telescope time with the GBT and one per half hour with MeerKAT. These TOAs enabled us to phase connect each pulsar back to 2005 using `TEMPO`, although the slightly fainter M28M required us to use the `DRACULA` software (Freire & Ridolfi 2018). The final timing solutions are provided in Table 1.

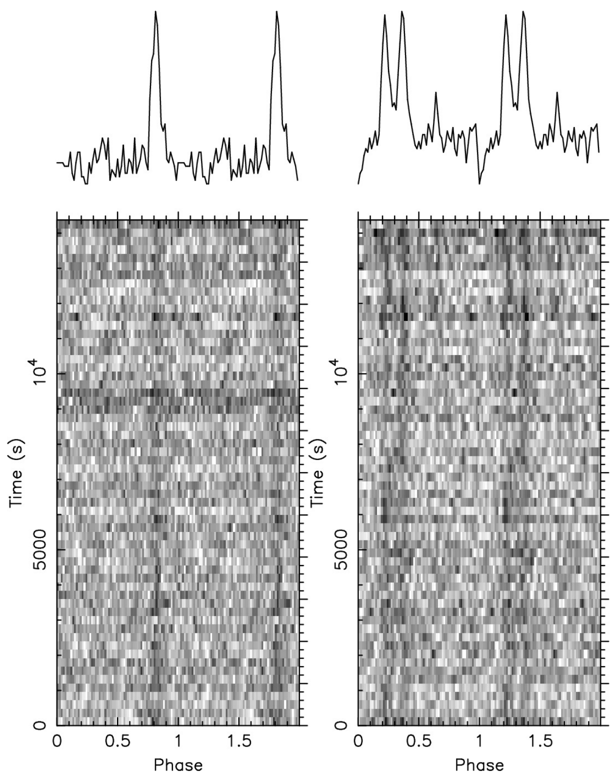

Figure 1. The best detections of M28M and M28N, respectively (left and right), from the MeerKAT TRAPUM observation on 2020 December 11. The pulses show two full rotations of the pulsar and the greyscale shows the intensity of the emission as a function of time.

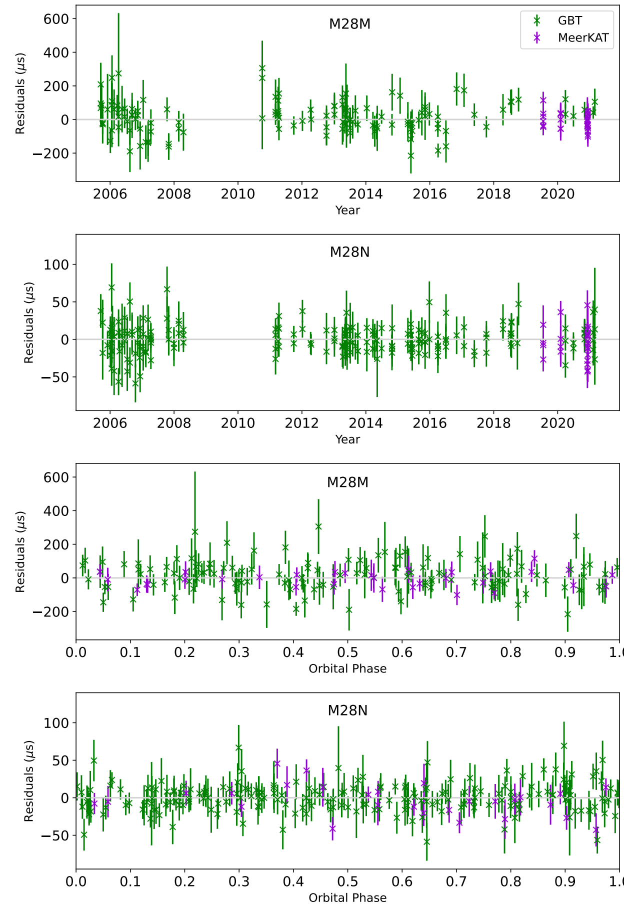

Figure 2. Timing residuals for M28M and M28N. Top two panels show timing residuals as a function of time. The bottom two tables show the residuals as a function of orbital phase.

3. DISCUSSION

There are many interesting implications from the timing of both M28M and M28N. Comparing the exotic binary population in M28 to the exotic binary population of other globular clusters reveals M28 as a particular hotbed of black widow and redback systems. The spin period derivative values of pulsars in globular clusters are often inaccurate due to effects of the gravitational field of the globular cluster. We used the upper limits on the orbital period derivatives of each pulsar to solve for various acceleration values in order to obtain a reasonable value for period derivative. We are able to corroborate the proper motion measurement by Gaia with our own measurements of the proper motion of M28 from the pulsar data. Finally we searched for possible evidence of x-ray emission of M28N in older. *Chandra* data. There is a chance that the spin period of M28M is 9.56 ms, twice the length of the period we show. The pulsar was actually discovered at this period but most of our subsequent observations have yielded the best results when analyzing the pulsar as a 4.78 ms rotator.

3.1. *Binaries*

Of the top 3 pulsar-populated globular clusters, M28 has the highest number of black widow systems for the amount of pulsars detected. Of the 27 known pulsars in 47 Tucanae, 6 are black widows and 3 are red-backs. Of the 39 known pulsars in Terzan 5, there are two black widows and 3 red-backs. In M28, of the 14 known pulsars there are 12 binaries, of them there are 5 black widows and 2 red-backs (Bégin 2006).

3.2. *Exotic Binary Populations in Globular Clusters*

In Bagchi et al. (2011), researchers utilized Monte Carlo simulations to predict the number of observable pulsars in 10 globular clusters using 6 different models. These models predicted M28 to have between 42 and 952 observable pulsars, with an average between the models of $\sim$316$\pm$60. Using this same table, we find that Terzan 5 has an average of 381 $\pm$ 40 pulsars and 47 Tuc an average of 158 $\pm$ 22 pulsars.

Using our knowledge of the numbers of black widow and red-back systems in these three clusters we can make a guess as to how many of these types of systems might be potentially observable. Note, we are only using these three clusters as we believe the sample size is large enough that the number of exotic systems can be seen as a *rough* trend. It must also be noted that there is a large discrepancy in the range of these models, but it is more useful to compare these results between clusters rather than between models.

Using these trends we find that M28 would have a potential 158 $\pm$ 28 black widow and red-back systems. Terzan 5 could have 35 $\pm$ 4 of these systems, and 47 Tuc could have 52 $\pm$ 7 systems. There are some reasons to believe that there exotic systems might appear more in M28 (or clusters with similar properties) such as the density of the cluster core, the rate of stellar interactions. We can conclude the this is not the result of bias in observation, and must be because of some characteristic of the cluster.

Another interesting result from our analyses of the new pulsars is the distinct lack of eclipses. Of the 5 black widow systems in M28, one shows an eclipse. These systems also do not show strong orbital variability, the lack of eclipse must mean that companion star is stable and there is not a lot of wind being ablated from it.

3.3. *Corrections for Pulse Period Derivative*

A common effect of discovering pulsars in globular clusters is measuring seemingly unphysical values of $\dot{P}$ compared to pulsars in the Galaxy. This contamination is a result of primarily the acceleration of the pulsar in the gravitational field of the cluster and leaves no vestige of the intrinsic period derivative in the observed period derivative (Phinney 1992). In Freire et al. (2017), in order to solve for the intrinsic period derivative, they use the equation

$$\frac{\dot{P}_{obs}}{P} = \frac{\dot{P}_{int}}{P} + \frac{\mu^2 d}{c} + \frac{a_{l,GC}}{c} + \frac{a_{l,gal}}{c} \quad (1)$$

$\dot{P}_{obs}$ is the observed spin-period derivative. $\dot{P}_{int}$ is the intrinsic spin-period derivative, which we aim to solve for. The second term on the right represents the Shklovskii effect (Shklovskii 1970) due to the motion of the pulsar in the plane of the sky. The third term represents the line-of-sight acceleration of the pulsar in the globular cluster. The fourth term represents the difference in acceleration between the solar system and the cluster in the field of the galaxy.

The Shklovskii effect may be solved for using the proper motion of the cluster and its distance, using proper motion data from Gaia (Vasiliev & Baumgardt 2021) which was 8.9 mas/year for the proper motion and 5.1 kpc for the distance. We found this term to be $9.82 \times 10^{-19}\,\mathrm{s}^{-1}$. The difference in acceleration may be solved for using the galactic coordinates of M28 and it's distance. We calculated the difference in acceleration term to be $9.91 \times 10^{-19}\,\mathrm{s}^{-1}$ (Freire et al. 2017) The line-of-sight acceleration may be solved for using

$$a_{l,GC} = \frac{\dot{P}_{b,obs}}{P_b} c - \mu^2 d - a \quad (2)$$

Where $\dot{P}_{b,obs}$ is the observed orbital period derivative. From this we may find the line-of-sight acceleration which we got to be $0.0012\,\mathrm{m/s^2}$. Putting all of this together gives a value for the intrinsic period derivative of M28M as -5.860×10^{-19} and M28N -1.306×10^{-20} which is more realistic than our previous value, 1.59×10^{-19}.

For M28M we assumed a magnetic field that gave a predicted $\dot{P}_b$ to 95% confidence (1.6σ) upper or lower limits of the period derivative. This gave upper limits on the magnetic field and $\dot{E}$ as well as a lower limit on the pulsar age.

3.4. *Proper Motion*

As measured by Gaia, M28 has a proper motion of 8.92(3) mas/yr. Our measured values of proper motion are consistent with the Gaia measurement of M28 (Vasiliev & Baumgardt 2021).

3.5. *Possible X-ray emission of M28N*

Pulsars can be bright X-ray sources. There have been detections of known radio pulsars in M28 in x-ray (Bogdanov et al. 2011). It is not enough to see a source in x-ray and decide it is a pulsar, even so, there are too many in the image of just the cluster center to make any such claim. However, we believe that we have detected M28N in a Chandra image (Bahramian et al. 2020) as we have found an x-ray count in the pixel closest to the known position of M28N. We continue to work on confirming this. We were not able to find M28M in the Chandra image, however.

4. CONCLUSION

After discovering two MSPs so far with this new MeerKAT data, which is only a bit more sensitive than previous state-of-the-art radio observatories, we expect that we could find dozens of MSPs with a more sensitive telescope within the limits of our present technology.

Studies such as this show the value of long-term monitoring projects of globular cluster pulsars. We hope that with future observations, and future discoveries we can use the TRAPUM and MeerTime data to phase connect like we did with the 2005 GBT data.

This the MeerTime and TRAPUM data we have, we continue to search the cluster for millisecond pulsars.

REFERENCES

Andersen, B. C., & Ransom, S. M. 2018, ApJL, 863, L13, doi: 10.3847/2041-8213/aad59f

Bagchi, M., Lorimer, D. R., & Chennamangalam, J. 2011, Monthly Notices of the Royal Astronomical Society, 418, 477–489, doi: 10.1111/j.1365-2966.2011.19498.x

Bagchi, M., Lorimer, D. R., & Wolfe, S. 2013, Monthly Notices of the Royal Astronomical Society, 432, 1303–1314, doi: 10.1093/mnras/stt559

Bahramian, A., Strader, J., Miller-Jones, J. C. A., et al. 2020, The Astrophysical Journal, 901, 57, doi: 10.3847/1538-4357/aba51d

Bailes, M., Jameson, A., Abbate, F., et al. 2020, PASA, 37, e028, doi: 10.1017/pasa.2020.19

Bégin, S. 2006, Master's thesis, University of British Columbia, doi: 10.14288/1.0085181

Bogdanov, S., van den Berg, M., Servillat, M., et al. 2011, ApJ, 730, 81, doi: 10.1088/0004-637X/730/2/81

Bussa, S., & VEGAS Development Team. 2012, in American Astronomical Society Meeting Abstracts, Vol. 219, American Astronomical Society Meeting Abstracts #219, 446.10

Camilo, F., Lorimer, D. R., Freire, P., Lyne, A. G., & Manchester, R. N. 2000, ApJ, 535, 975, doi: 10.1086/308859

Danner, R., Kulkarni, S. R., & Thorsett, S. E. 1994, ApJL, 436, L153, doi: 10.1086/187655

DuPlain, R., Ransom, S., Demorest, P., et al. 2008, in Advanced Software and Control for Astronomy II, ed. A. Bridger & N. M. Radziwill, Vol. 7019, International Society for Optics and Photonics (SPIE), 496 – 505, doi: 10.1117/12.790003

Freire, P. C. C., & Ridolfi, A. 2018, MNRAS, 476, 4794, doi: 10.1093/mnras/sty524

Freire, P. C. C., Ridolfi, A., Kramer, M., et al. 2017, MNRAS, 471, 857, doi: 10.1093/mnras/stx1533

Kaplan, D., Escoffier, R., Lacasse, R., et al. 2005, Publications of the Astronomical Society of the Pacific, 117, 643. http://www.jstor.org/stable/10.1086/430368

Lyne, A. G., Brinklow, A., Middleditch, J., Kulkarni, S. R., & Backer, D. C. 1987, Nature, 328, 399, doi: 10.1038/328399a0

Papitto, A., Ferrigno, C., Bozzo, E., et al. 2013, Nature, 501, 517, doi: 10.1038/nature12470

Phinney, E. S. 1992, Philosophical Transactions of the Royal Society of London Series A, 341, 39, doi: 10.1098/rsta.1992.0084

Ransom, S. M. 2001, PhD thesis, Harvard University

Ransom, S. M. 2008, in Dynamical Evolution of Dense Stellar Systems, ed. E. Vesperini, M. Giersz, & A. Sills, Vol. 246, 291–300, doi: 10.1017/S1743921308015810

Ransom, S. M., Hessels, J. W. T., Stairs, I. H., et al. 2005, Science, 307, 892, doi: 10.1126/science.1108632

Ridolfi, A., Gautam, T., Freire, P. C. C., et al. 2021, MNRAS, doi: 10.1093/mnras/stab790

Roberts, M. S. E. 2013, in Neutron Stars and Pulsars: Challenges and Opportunities after 80 years, ed. J. van Leeuwen, Vol. 291, 127–132, doi: 10.1017/S174392131202337X

Shklovskii, I. S. 1970, Soviet Ast., 13, 562

Vasiliev, E., & Baumgardt, H. 2021, Gaia EDR3 view on Galactic globular clusters. https://arxiv.org/abs/2102.09568

Table 1. New MeerKAT Pulsars

Parameter	Value(Error)	Value(Error)
Pulsar Name	J1824-2452M	J1824-2452N
Right Ascension (RA, J2000)	$18^{\rm h}\,24^{\rm m}\,33\overset{\rm s}{.}1835(5)$	$18^{\rm h}\,24^{\rm m}\,33\overset{\rm s}{.}1418(12)$
Declination (DEC, J2000)	$-24^\circ\,52'\,08\overset{''}{.}2(23)$	$-24^\circ\,52'\,11\overset{''}{.}89(3)$
Proper Motion Right Ascension (mas/yr)	0.0(1.4)	0.5(0.3)
Proper Motion Declination (mas/yr)	−23(28)	−15(6)
Pulsar Period (ms)	4.7842842982785(7)	3.35287243686099(10)
Pulsar Frequency (Hz)	209.01767906222(3)	298.251728579395(9)
Frequency Derivative ($\mathrm{Hz\,s^{-1}}$)	$-5.36572(12)\times10^{-15}$	$-1.416227(3)\times10^{-14}$
Frequency Second Derivative ($\mathrm{Hz\,s^{-2}}$)	$-1.4(4)\times10^{-26}$	$-9(1)\times10^{-27}$
Reference Epoch (MJD)	56450	56450
Dispersion Measure ($\mathrm{pc\,cm^{-3}}$)	119.352(11)	119.321(3)
Orbital Period (days)	0.2425192190(14)	0.19849331510(11)
Orbital Period Derivative	3.1(1.6) x 10^{-12}	0.62(14) x 10^{-12}
Projected Semi-Major Axis (lt-s)	0.032463(8)	0.0497303(16)
Time of Ascending Node	56451.272704(15)	56451.2896713(15)
Properties of Fit		
Span of Timing Data (MJD)	53629−59274	53629−59274
Number of TOAs	161	230
RMS TOA Residual (μs)	71.11	16.45
Derived Parameters		
Mass Function ($M_\odot$)	$6.245(4)\times10^{-7}$	$3.3516(3)\times10^{-6}$
Min Companion Mass ($M_\odot$)	≥ 0.011	≥ 0.019
Pulsar Magnetic Field (G) †	$> 3\times10^{8}$	3.6×10^{8}
Pulsar Age (years) †	$< 3\times10^{9}$	1.4×10^{9}
Pulsar $\dot{E}$ (erg/s) †	$> 8\times10^{33}$	4.0×10^{34}
Flux Density at 2 GHz (mJy)	0.06	0.06
Angular Offset of Cluster Center (mas) ‡	5.092	3.464
Total Proper Motion	10(22)	14(7)

Note—Numbers in parentheses represent 1-σ uncertainties in the last digit. The timing solution was determined using `TEMPO` with the DE440 (Ridolfi et al. 2021) Solar System Ephemeris and the DD binary model. The time system used is Barycentric Dynamical Time (TDB), referenced to TT via BIPM. The minimum companion mass was calculated assuming a pulsar mass of $1.4\,M_\odot$. † Here we assumed a magnetic field that gave a predicted $\dot{P}_b$ to 95% confidence as described in §3.2, a lower limit on the age and an upper limit on the $\dot{E}$ 3.2. ‡ Values of proper motion consistent with values measured by Gaia 3.4.